XRD and electron diffraction synergies for textured thin films structure investigation

Cite as: AIP Conference Proceedings **2131**, 020028 (2019); https://doi.org/10.1063/1.5119481
Published Online: 29 July 2019

Rostislav Medlín, Pavol Šutta, and Petr Novák

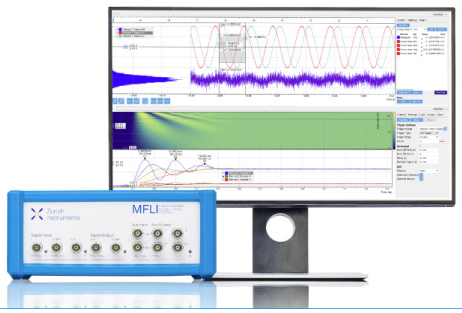

XRD and Electron Diffraction Synergies for Textured Thin Films Structure Investigation

Rostislav Medlín [1, a)], Pavol Šutta [1)], and Petr Novák [1)]

[1] *New Technologies Research Centre, University of West Bohemia, Univerzitní 8, 306 14 Pilsen, Czech Republic*

[a)] Corresponding author: medlin@ntc.zcu.cz

Abstract. In this study, Titanium (Ti) doped zinc oxide (ZnO) thin films were successfully deposited by reactive magnetron co-sputtering in a reactive mode from metallic targets with different Ti concentrations (up to 9 at % of Ti) at relatively low temperatures (~ 200 °C) to investigate changes of the microstructure. Detailed crystal and local atomic structures of the films were characterized via X-ray diffraction (XRD) and on cross-section X-TEM samples on HR-TEM together with electron diffraction (ED) patterns. Obtained results revealed that substitution of Zn sites by Ti ions degrade original hexagonal wurtzite phase of ZnO with increasing doping concentrations through ZnO:Ti-like to $ZnTiO_3$-like materials with a small amount of TiO_2 (anatase phase). This study clearly suggests that investigations of textured samples by two geometries of XRD together with 1D and 2D XRD detectors have its limitations and cooperation with X-TEM ED results can lead to better understanding of highly-textured materials.

INTRODUCTION

Nano-materials are used nowadays in environmental, biomedical, energy conversion, food safety, security applications etc. Nano-structured ZnO have enormous application potential as versatile material for optoelectronic, solar cells and spintronics for its wide direct band-gap (3.37 eV) and high transparency, non-noxious and excellent chemical stability and also for low-cost fabrication. As a transparent semiconductor material, ZnO is widely used in thin film transistors (TFT), LEDs, flat panel displays etc.

Zinc oxide generally crystallized in the hexagonal wurtzite structure in ambient condition [1]. However, structural properties of the material could be changed by doping elements to get remarkable changes of the structure and optical, electrical, mechanical or other properties. In our case we prepared Ti doped ZnO thin films (up to 9 at% of Ti) by reactive magnetron co-sputtering from pure Zn and Ti targets (99.9% in purity) in Ar+O2 atmosphere. Thin films had highly textured structure and XRD investigation together with TEM ED showed interestingly complementary information. Only utilization of different XRD geometries together with X-TEM prepared samples ED patterns allowed to interpret complex characterization of thin films microstructure.

EXPERIMENTAL PROCEDURE

Zinc oxide films were deposited on [001] oriented single-crystalline silicon substrates by RF reactive sputtering (with RF frequency of 13.56 MHz) using a BOC Edwards TF 600 electron beam evaporation and sputtering system. Film thickness varied from ~ 200 to 500 nm.

Elemental analysis was carried out by energy dispersive X-ray spectroscopy (EDS) on SEM (JEOL JSM-7600F) equipped with EDS detector (X-Max, Oxford Instruments). XRD measurements were carried out on an automatic X-ray powder diffractometer X'Pert Pro equipped with an ultrafast linear semiconductor detector PIXcel and with a point detector. As an X-ray source the CuKα radiation (λ = 0.154178 nm) has been used.

For thin films structure characterization two different XRD geometries have been used: Symmetric Bragg-Brentano (ϑ-ϑ) and asymmetric Seemann-Bohlin (ω-2ϑ) geometries (Fig. 1 left). Both geometries have given diffraction from different lattice planes. While Bragg-Brentano geometry gives diffraction from the planes parallel

Applied Physics of Condensed Matter (APCOM 2019)
AIP Conf. Proc. 2131, 020028-1–020028-7; https://doi.org/10.1063/1.5119481
Published by AIP Publishing. 978-0-7354-1873-8/$30.00

to the surface, the Seemann-Bohlin geometry gives diffraction from the planes deflected from the sample surface by $\delta = \vartheta - \omega$ angle. Incident angle ω is usually much less than 10 degrees and is kept fixed during the experiment. XRD patterns were recorded from 25 to 65° (ϑ-ϑ geometry) and 25–75° (ω-2ϑ geometry) [2]. To achieve the basic microstructure parameters of the films, line profile analysis was performed by procedures based on a Voigt function [3, 4].

Cross section TEM (X-TEM) samples prepared by JEOL Cryo Ion Slicer were investigated by High-resolution transmission electron microscopy (HRTEM) JEOL JEM 2200FS operated at 200 kV. Images were recorded on a Gatan 2048×2048 pixels CCD camera using the Digital Micrograph SW package.

Selected Area Electron Diffraction (SAED) patterns were treated by Process Diffraction [5]. Data treatment included circle integration of intensities of SAED data from TEM and calibration of integrated data intensity peaks with used Camera Length (CL) for comparison and indexation purposes with Powder Diffraction File (PDF) database from JCPDS (ICDD) as a standard comprehensive database of material structures from X-Ray Diffraction (XRD) patterns. Image of planes investigated in cross-section sample of thin film by TEM Electron Diffraction is in Fig. 1- right. Diffraction conditions in the thin film are accomplished only to planes, which have one direction parallel to the electron beam.

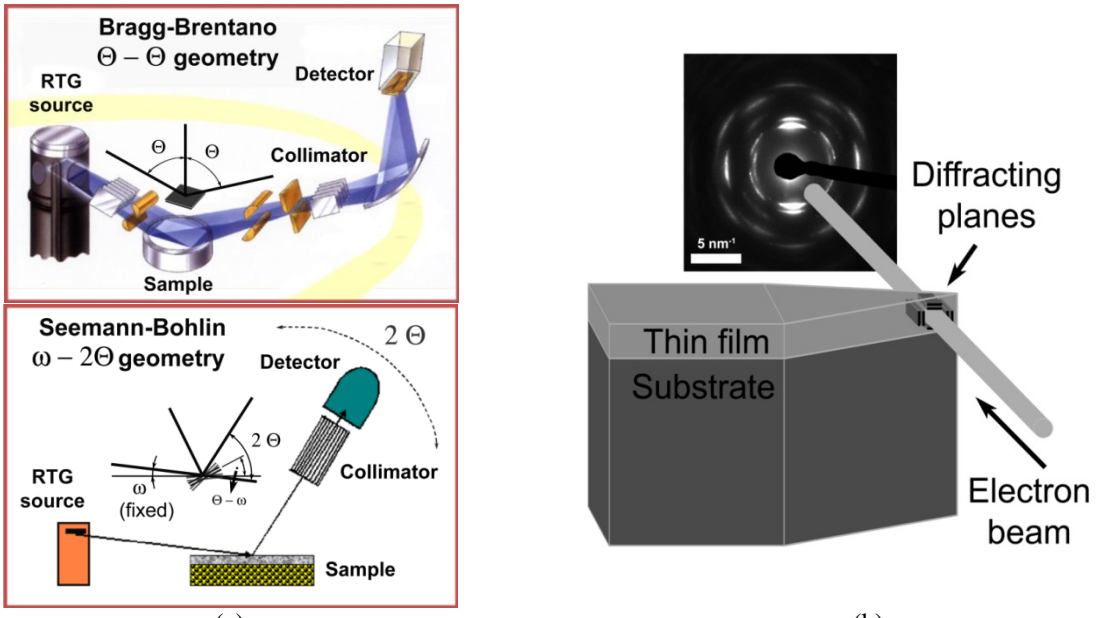

FIGURE 1. X-Ray geometries with planes contributing to diffraction: Bragg-Brentano (ϑ-ϑ) – top, Seeman-Bohlin (ω-2ϑ) – down (a). Planes contributing to electron diffraction patterns for thin films cross-section samples (b).

RESULTS AND DISCUSSION

X-ray diffraction analysis indicated that all films are polycrystalline with strong preferred orientation of their crystallites in [001] direction for ZnO-like films and in [104] direction for $ZnTiO_3$-like films, perpendicular to sample surface taken from symmetric geometry. Nevertheless, the ω-2ϑ geometry has given also the other preferred orientations of (002) and (104) lattice planes (See Fig. 2) deflected from the film surface at about 17 and 16 degrees respectively. XRD patterns taken from the films with different Ti content are presented in Fig. 2, where shift of the observed line positions are clearly seen from the ZnO wurtzite structure to $ZnTiO_3$ hexagonal perovskite structure. Strong preferred orientation of crystallites (texture) by XRD patterns is also evident. Two different directions of crystallite preferred orientations are demonstrated in ω-2ϑ geometry. Reference XRD patterns from ZnO powder with randomly oriented crystallites for both symmetric (ϑ-ϑ) and asymmetric (ω-2ϑ) geometries are presented in Fig. 3.

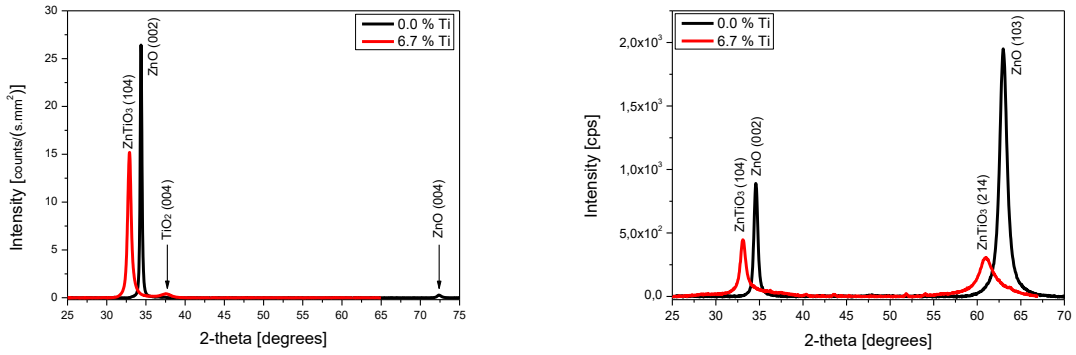

(a) (b)

FIGURE 2. XRD patterns for ZnO:Ti thin films with 0 and 6.7 at % Ti content for both geometries.

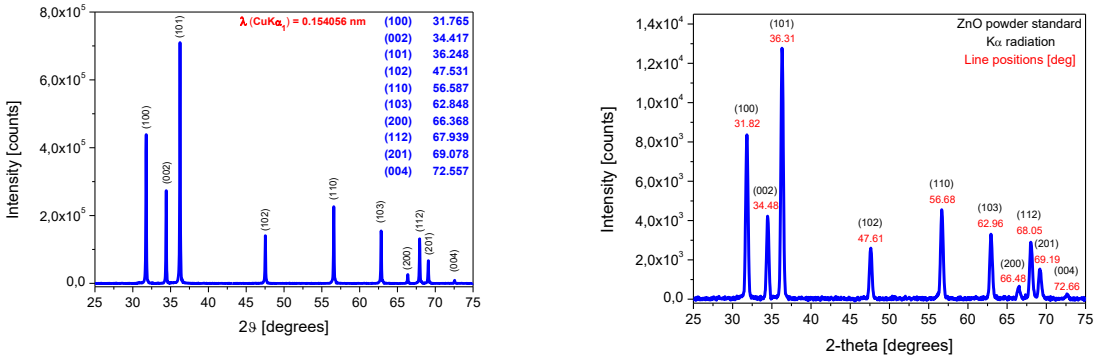

(a) (b)

FIGURE 3. XRD patterns for ZnO powder standard for both geometries.

Size-strain parameters results were obtained from the line profile analysis using an integral breadth of the line profile $\beta = I_{int}/I_0$, where I_{int} is the integrated intensity of the line profile and I_0 is the intensity in the peak position. Average crystallite dimensions $\langle D \rangle$ in direction perpendicular to the thin film surface and micro-strains $\langle \varepsilon \rangle$ are presented in Table 1. As can be seen in table, crystallite size generally becomes smaller with increasing Ti concentration in the films. Every $\langle D \rangle$ value has its integral intensity (last column in table), which means how much volume analysed is occupied by the crystallites having this particular crystallite size value. Diffraction lines for some samples have two different crystallite size values. It means that there is a bi-modal distribution of crystallite sizes.

TABLE 1. Size-strain results obtained from XRD analysis (ϑ-ϑ geometry).

Sample		**XRD parameters**			
Ti [at %]	(h k l)	2ϑ [deg]	<D> [nm]	<ε> [-]	Intensity [%]
0	(002) ZnO	34.351	84	0.0023	100
2.4	(002) ZnO	33.891	52	0.0023	85
		34.092	17	0.0029	6
	(101) ZnO	35.886	11	0.0018	9
6.7	(104) $ZnTiO_3$	32.871	48	0.0066	72
		33.171	13	0.0210	21
	(004) TiO_2	37.438	8	0.0160	7
8.7	(104) $ZnTiO_3$	32.569	19	0.0094	72
		32.883	8	0.0260	22
	(004) TiO_2	37.838	17	0.0170	6

TEM results are partially in Fig. 4 and 5, where HR-TEM investigations of thin films are presented together with Electron Diffraction patterns. Particle size in Fig. 4 nicely corresponds with XRD results, ED patterns together with HR-TEM show strongly presence of disorientations of small crystallites. Rate of disorientations grows with Ti content and can be clearly seen on ED patterns. Inter-planar distances also grow with Ti content, as indicated XRD results in Fig. 2 and TEM in Fig. 5 bottom.

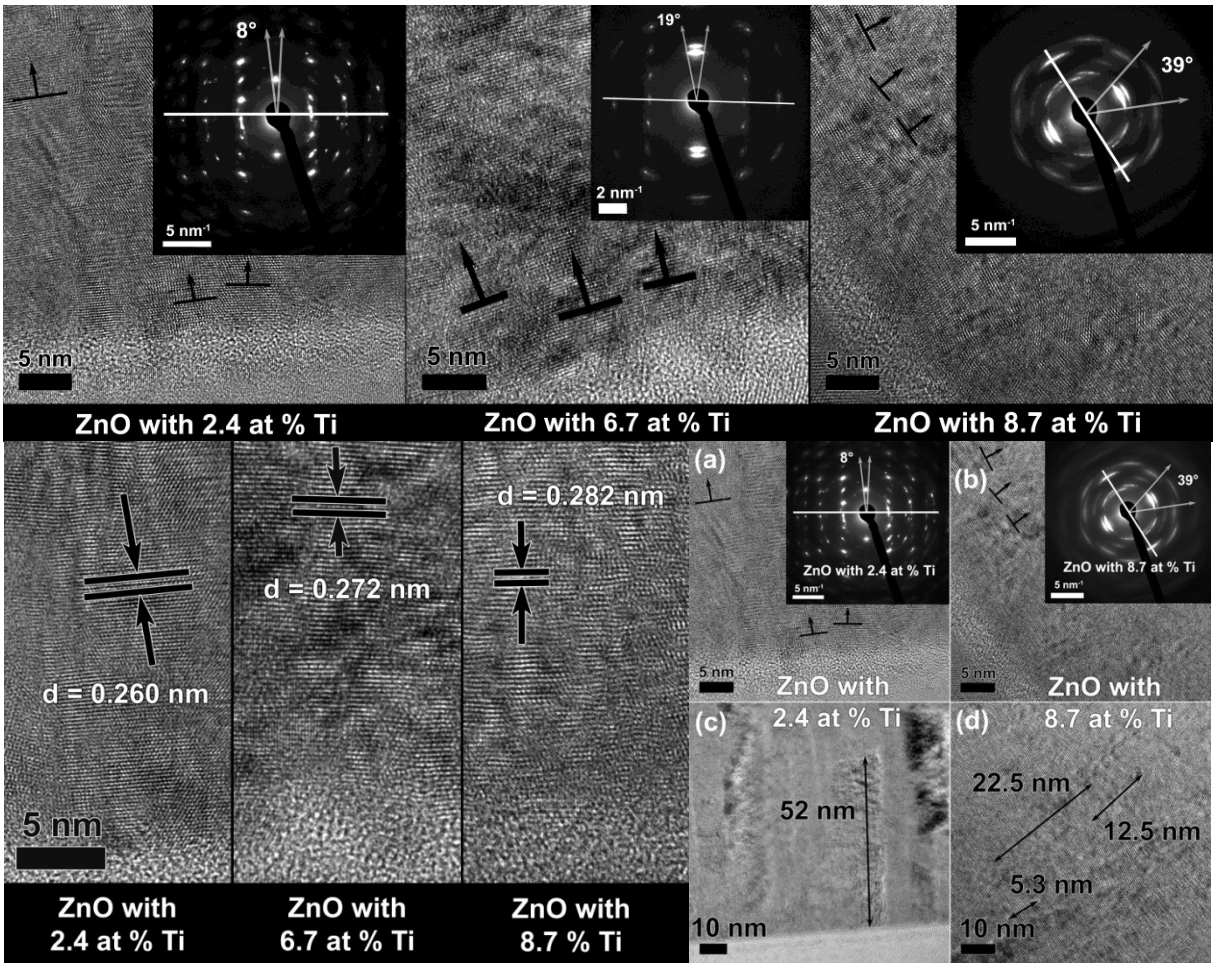

FIGURE 4. HR-TEM and electron diffraction patterns from X-TEM ZnO:Ti thin films with 2.4, 6.7 or 8.7 at % Ti respectively with crystallite planes miss-orientation indicated (top) and inter-planar distance change with Ti content (bottom).

Comparison of ED with XRD results are in Fig. 5. As for XRD ϑ-ϑ geometry contributes only planes indicated in Fig. 1 – left, for comparison of both diffractions we have to consider plane directions contribute to both geometries and also plane directions as it contributes to ED pattern. Planes parallel to the surface and to the electron beam will result in ED patterns as intensity according line in direction perpendicular to sample surface from primary beam position (have to be measured separately) and should be compared with XRD ϑ-ϑ pattern which is also indicated in the figure. Scattering Vector in ED could be recalculated to Cu 2ϑ degrees through d values, graph of relationship between electron diffraction Scattering Vector = $2\pi/d$ [1/nm] and XRD diffraction 2ϑ angle for Cu radiation is in Fig. 6. In Fig. 5 there are lines marked in one side with Scattering Vector values and on other side with Cu 2ϑ degrees by this relationship. For XRD ω-2ϑ geometry is also possible to compare intensity, line of contributed planes in ED is also indicated in the image, taken into care inclination of contributed planes from parallel direction to ω-ϑ angle.

The only planes corresponding with indicated planes in Fig. 4 contribute to XRD results for both geometries. As can be seen in Fig. 5, strong texture of thin films do not allow XRD to see all presented d values belonging to thin films. Circular integration of ED with Process Diffraction [5] allow us to compare intensities belonging to all d

values presented in ED with JCPDS database *d* values correspond to different phases indicated from XRD measurements as it can be seen in Fig 7.

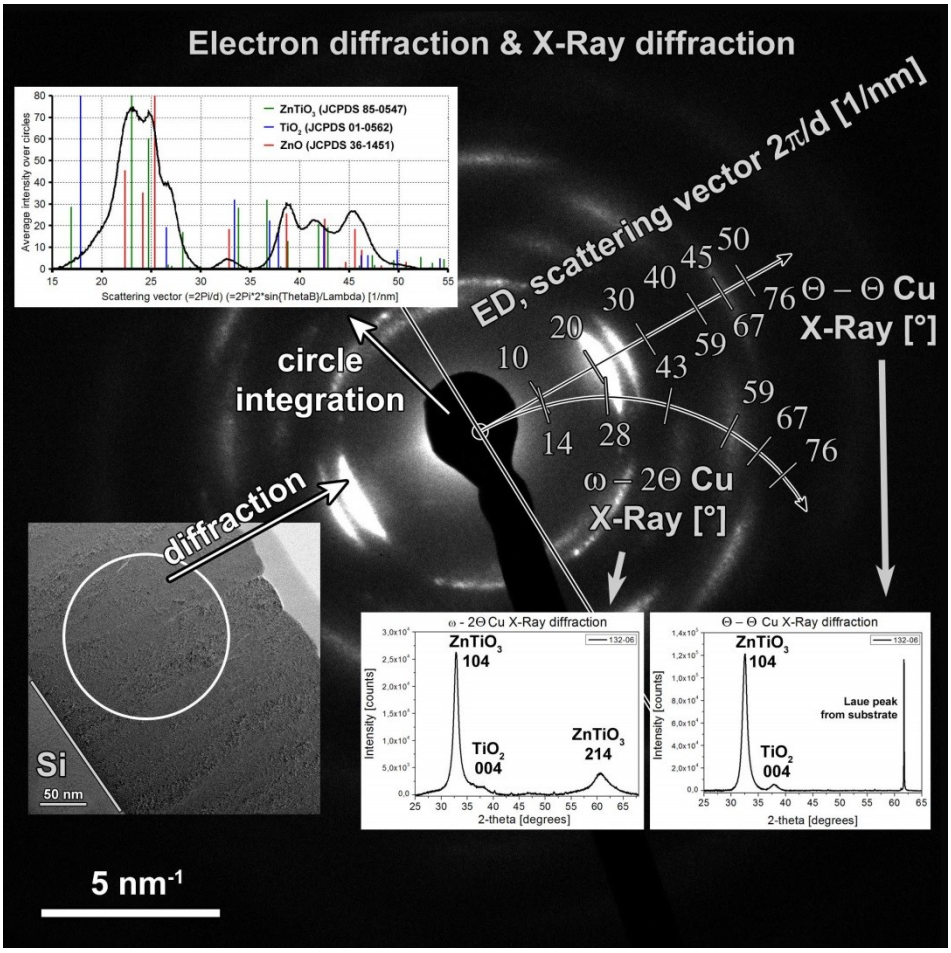

FIGURE 5. HR-TEM and electron diffraction patterns from X-TEM ZnO:Ti thin films.

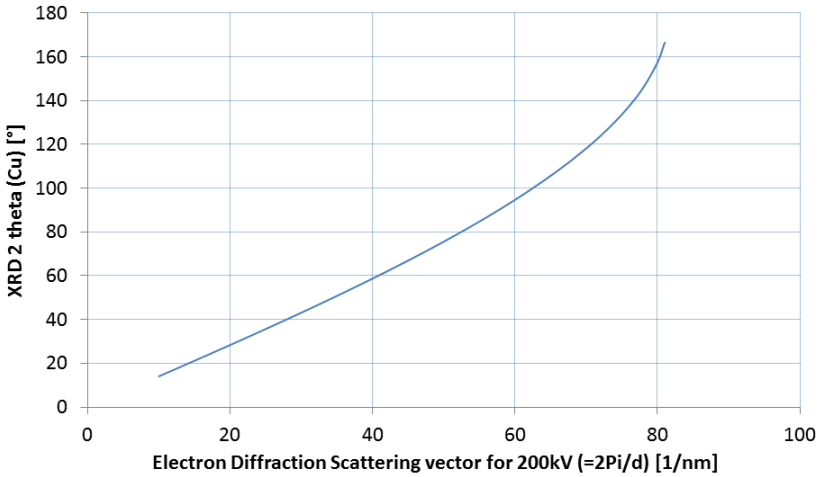

FIGURE 6. Relationship between Electron Diffraction Scattering Vector for 200 kV and 2Θ angle for Cu radiation.

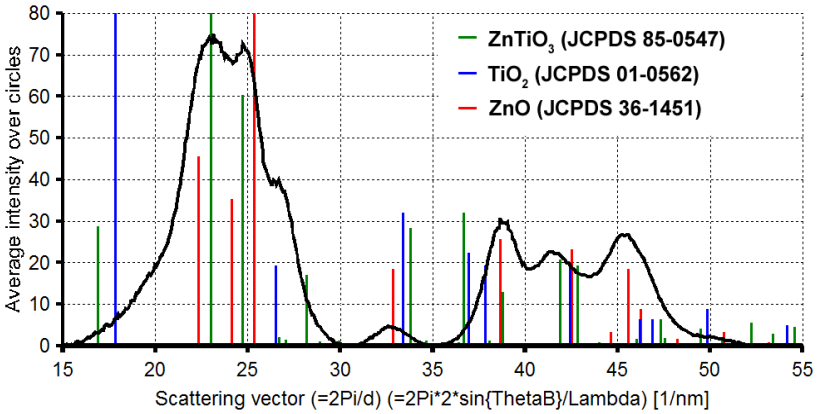

FIGURE 7. ED processed with PD [2] with indicated JCPDS database lines for XRD phases.

Both results show information about texture of investigated thin films, while ED patterns can be used as indication of pole figure for single line intensity dependency on inclination of planes from direction perpendicular to the surface plane. For example for XRD is not possible to see $ZnTiO_3$ diffraction from plane 214 on current ϑ-ϑ geometry. To avoid detector damage from the silicon substrate diffracted line it is also not possible to see XRD data on ϑ-ϑ geometry above 65° of 2ϑ angle, while presence on ED is clear.

We have to consider dynamic diffraction effects as they modify ED patterns, so we have to rely on XRD results, as they indicate presence of $ZnTiO_3$ phase. With that information it is possible to mask FFT of HR-TEM picture on proper inter-planar distances and show in different colours results of reverse FFT process. For some inter-planar distances connected to different phases indicated from XRD FFT processing of HR-TEM picture of ZnO:Ti thin film with 8.7 at % Ti were done in Fig. 8.

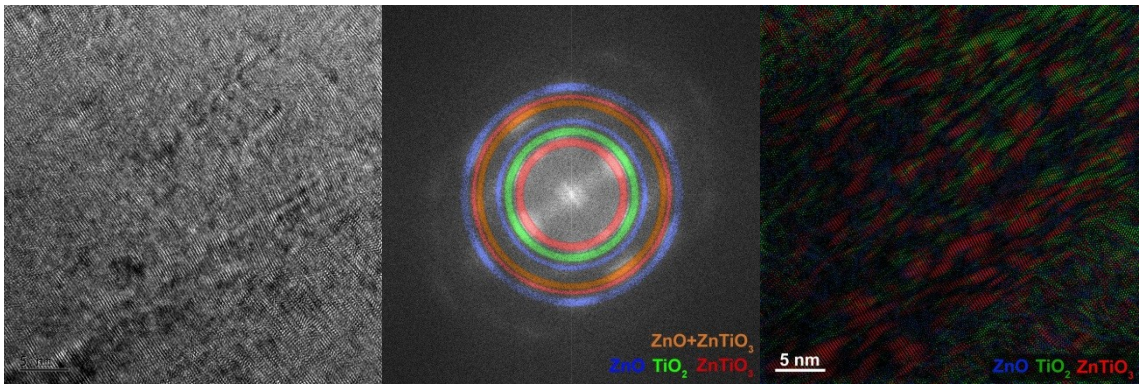

FIGURE 8. FFT process of HR-TEM image with inter-planar distances of different phases marked and indicated with colours.

CONCLUSIONS

This paper is focussed on explanation of the structure (phase) transformation from ZnO films to $ZnTiO_3$ films prepared by reactive magnetron co-sputtering when titanium content in films has increased. The structure of prepared films gradually changed from the well crystalline columnar structure with two strong preferred orientations of pure ZnO wurtzite structure in [001] direction perpendicular and deflected at 17 degrees to the substrate surface, to nano-crystalline $ZnTiO_3$ hexagonal structure with two preferred orientations in [104] direction to the film surface and deflected from the film surface at 16 degrees. A small amount of TiO_2 (anatas phase) was also observed. We found out that presence of two different preferred crystallite orientations in the ZnO films deposited on substrates in [001] direction is typical for the films, which are prepared by reactive magnetron co-sputtering in $Ar+O_2$ atmosphere from the metallic targets compared to the ZnO films deposited from the ceramic ZnO targets, which have only one [001] preferred crystallite orientation perpendicular to the film surface. Crystalline optical materials with hexagonal lattice structure have anisotropic optical properties. Polycrystalline materials with randomly oriented crystallites in

space lose their anisotropy, but when their crystallites are preferably orientated in some direction, they are optically anisotropic again. It means that a double refraction can be observed when light is passing through such materials. It is not evident whether this fact plays important role in thin films utilization, nevertheless, double refraction is one of the typical properties of anisotropic optical materials.

The phase transformation observed has been examined by X-ray diffraction and high resolution TEM and electron diffraction, where XRD is a global method (giving information from relatively large volume), on the other hand, TEM is a local method (giving information from a very small volume). Both experimental techniques confirmed the structure (phase) transformation and furthermore they complemented each other. The best approximation to the $ZnTiO_3$ phase was obtained for 6.7 at % of Titanium content in the films analysed. Reduction of coherently diffracting domains (crystallites) and enlargement of micro-strains (Tab. 1) established, when Titanium increased, has on conscience probably the fact that there is some redundant amount of oxygen atoms in the interstitial positions, which deforms the lattice structure. Because there are still some unclarities in relations between the structure of films analysed and parameters of technology used, it is necessary to perform additional experiments.

ACKNOWLEDGMENTS

The result was developed within the CENTEM project, reg. no. CZ.1.05/2.1.00/03.0088, co-funded by the ERDF as part of the Ministry of Education, Youth and Sports OP RDI programme and, in the follow-up sustainability stage, supported through CENTEM PLUS (LO1402) by financial means from the Ministry of Education, Youth and Sports under the ”National Sustainability Programme I.” and European Regional Development Fund (ERDF), project CEDAMNF, reg. no. CZ.02.1.01/0.0/0.0/15_003/0000358.

REFERENCES

1. K. Ellmer, A. Klein, B. Rech: *Transparent conductive zinc oxide basics and applications in thin film solar cells*. Berlin: Springer; 2008.
2. S. Rajendran, P. Šutta, P. Novák, M. Netrvalová, A. Hendrych, O. Životský: *In-situ X-ray diffraction studies and magneto-optic Kerr effect on RF sputtered thin films of BaTiO3 and Co, Nb co-doped BaTiO3*. Ceramics International 42 (2016), p. 3882-3887. ISSN: 0272-8842
3. J. I. Langford: *The use of the Voigt function in determining microstructural properties from diffraction data by means of pattern decomposition*. In Accuracy in Powder Diffraction II, Gaithersburg, USA June 1992.
4. R. Delhez, Th. H. de Keijser and E.J. Mittemeijer*: Determination of Crystallite Size and Lattice Distortions through X-ray Diffraction Line Profile Analysis*. Fresenius Z Anal Chem (1982) **312**, 1-16.
5. J. L. Lábár: *Consistent indexing of a (set of) SAED patterns with the Process Diffraction program*, Ultramicroscopy, **103** (2005) 237-249. M. P. Brown and K. Austin, *The New Physique* (Publisher Name, Publisher City, 2005), pp. 25–30.